

Promoting effects of calponin 3 on the growth of diffuse large B-cell lymphoma cells

XIAOJING XING¹, MEICHEN LIU¹, XUGUANG WANG², QIANXUE GUO¹ and HONGYUE WANG³

¹Department of Hematology and Breast Cancer, Cancer Hospital of Dalian University of Technology (Liaoning Cancer Hospital and Institute), Shenyang, Liaoning 110042; ²Department of Pathology, Shenyang Medical College, Shenyang, Liaoning 110034; ³Department of Scientific Research and Academic, Cancer Hospital of Dalian University of Technology (Liaoning Cancer Hospital and Institute), Shenyang, Liaoning 110042, P.R. China

Received August 31, 2022; Accepted December 23, 2022

DOI: 10.3892/or.2023.8483

Abstract. Diffuse large B-cell lymphoma (DLBCL) is one of the most common types of lymphoma. Calponin 3 (CNN3) is a thin filament-associated protein previously known to regulate smooth muscle contraction. Recent evidence illustrates its involvement in carcinogenesis; however, its roles in DLBCL remain unknown. CNN3 was found to be highly expressed in DLBCL specimens according to the online Gene Expression Profiling Interactive Analysis data. The aim of the present study was to investigate the roles of CNN3 in the progression of DLBCL. *In vitro*, the ectopic expression of CNN3 promoted the proliferation and G1/S transition of DLBCL cells, while its silencing led to opposite alterations. A similar tumor-promoting role of CNN3 was also demonstrated by injecting nude mice with DLBCL cells over- or underexpressing CNN3. The results of dual-luciferase reporter and chromatin immunoprecipitation assays revealed that forkhead box O3 (FOXO3), a known tumor suppressor in DLBCL, bound to the CNN3 promoter at -1955/-1948 and -1190/-1183, and suppressed the transcription of CNN3. The alterations induced by FOXO3 were partly blocked by CNN3 overexpression. On the whole, the present study demonstrates that CNN3, whose transcriptional activity is negatively regulated by FOXO3, contributes to the malignant behavior of DLBCL cells. The findings of the present study may provide novel diagnostic or therapeutic insight for DLBCL in clinical practice.

Introduction

Lymphoma is a type of malignancy originating from the lymphatic-hematopoietic system, which mainly includes

Hodgkin's lymphoma and non-Hodgkin's lymphoma, the latter accounting for 80-90% of all lymphoma cases (1). Non-Hodgkin's lymphoma is derived from natural killer cells, or B/T-lymphocytes. Diffuse large B-cell lymphoma (DLBCL) is the most common type, and accounts for 30-40% of non-Hodgkin's lymphomas (2). DLBCL primarily occurs in the lymph nodes, and also in extranodal tissues, including the gastrointestinal tract, bone and central nervous system (3). Due to its heterogeneity, there are differences in the clinical presentation of DLBCL. The diagnosis of DLBCL cases is generally made from the pathological determination of excisional lymph nodes (2,4). Therefore, the development of sensitive and specific markers for the clinical diagnosis of DLBCL would be beneficial.

Calponin 3 (CNN3) is a thin filament-associated protein, implicated in the modulation and regulation of smooth muscle contraction. Initially, CNN3 was revealed to inhibit the Mg ATPase activity of smooth muscle myosin (5,6). Subsequent evidence demonstrated that CNN3 induced actin polymerization and hindered depolymerization of actin filaments (7). Furthermore, CNN3 is also expressed in the brain, in order to regulate the dendritic spine plasticity of hippocampal neurons, with the systemic knockout of CNN3 resulting in embryonic and neonatal lethality, due to developmental defects of the central nervous system (8,9). Additionally, CNN3 regulates the actin cytoskeleton rearrangement of choriocarcinoma cells (10), suggesting its effects on tumorigenesis. Recent reports have demonstrated the cancer-promoting roles of CNN3. For instance, the ectopic expression of CNN3 promotes the growth and metastasis of cervical cancer cells (11). CNN3 enhances the invasion and drug resistance of digestive tract cancer cells, including colon cancer and gastric cancer cells (12,13). However, the effects of CNN3 on hematopoietic malignancies remain unknown. In the present study, gain- and loss-of-function assays were performed to confirm the roles of CNN3 in DLBCL cells.

Additionally, forkhead box O3 (FOXO3) has been reported to function as a tumor suppressor in various cancer types, including gastric (14), prostate (15) and lung cancer (16). A recent study reported that the silencing of FOXO3 promoted the proliferation and inhibited the apoptosis of DLBCL cells (17). As a transcription factor, FOXO3 simultaneously functions as

Correspondence to: Dr Xiaojing Xing, Department of Hematology and Breast Cancer, Cancer Hospital of Dalian University of Technology (Liaoning Cancer Hospital and Institute), 44 Xiaoheyan Road, Shenyang, Liaoning 110042, P.R. China
E-mail: xingxiaojing@cancerhosp-ln-cmu.com

Key words: diffuse large B-cell lymphoma, calponin 3, forkhead box O3, proliferation, apoptosis

a transcription enhancer and suppressor. For instance, FOXO3 promotes the transcription of BH3 interacting domain death agonist and cathepsin L (18,19), and inhibits the transcription of integrin $\beta 1$ and interleukin 10 (20,21).

The data of the present study demonstrated that the expression of CNN3 was downregulated by FOXO3, suggesting that FOXO3 may function by regulating CNN3 in DLBCL cells. To verify this hypothesis, the effects of FOXO3 and CNN3 were evaluated in DLBCL cells, and rescue experiments were also performed in the present study.

Materials and methods

Cell culture and treatment. The human DLBCL cell lines, DB (cat. no. CL-0645, Procell Life Science & Technology Co., Ltd.) and SU-DHL-4 (cat. no. CC1606, Guangzhou Cellcook Biotech Co., Ltd.), were cultured with RPMI-1640 (Beijing Solarbio Science & Technology Co., Ltd.) containing 10% fetal bovine serum (FBS) at 37°C with 5% CO₂, and 293T cells (cat. no. ZQ0033, Shanghai Zhong Qiao Xin Zhou Biotechnology Co., Ltd.) were cultured with DMEM (Wuhan Servicebio Biotechnology Co., Ltd.) supplemented with 10% FBS.

Cell transfection. To control the expression of CNN3 and FOXO3, the coding sequence of CNN3 or FOXO3 was cloned into pcDNA3.1 vector (Shaanxi Youbio Technology Co., Ltd.). The short interference RNA (siRNA), short hairpin RNA (shRNA) targeting CNN3 and their negative control (NC) sequences were synthesized by General Biology Co., Ltd., and shRNA was inserted into pRNA-H1.1 (General Biology Co., Ltd.). All siRNA and shRNA sequences are presented in Table I. The DB or SU-DHL-4 cells were transfected with plasmid or RNA (original concentration: Plasmid, 0.1 $\mu\text{g}/\mu\text{l}$; siRNA, 0.01 nmol/ μl) using Lipo8000 reagent (Beyotime Institute of Biotechnology) 2.5 μg plasmid or 100 pmol siRNA for 2-3 $\times 10^5$ cells in 200 μl solution) for 4-6 h. Subsequently, 20 h following transfection, the cells were used in subsequent analyses. The siRNA and shRNA sequences are presented in Table I.

It was observed that the DB cells grew slightly more rapidly than the SU-DHL-4 cells; thus, the DB cells were used in the xenograft experiment. In order to obtain cells stably overexpressing CNN3 or cells in which CNN3 was silenced, DB cells transfected with overexpression or knockdown vector were treated with G418 (200 $\mu\text{g}/\text{ml}$; Beijing Solarbio Science & Technology Co., Ltd.) for ~6 weeks. The cells remaining alive were considered as CNN3-stably-overexpressing or -silenced DLBCL cells.

Reverse transcription-quantitative PCR (RT-qPCR). Total RNA extraction was performed using TRIpure lysis buffer (Beijing BioTeke Corporation Co., Ltd.) and trichloromethane (Shanghai GenePharma Co., Ltd.), and purified with isopropanol and 75% ethanol (Shanghai GenePharma Co., Ltd.). Following quantification with a NANO2000 spectrophotometer (Thermo Fisher Scientific, Inc.), the RNA was reverse transcribed into cDNA using BeyoRT II M-MLV reverse transcriptase (Beyotime Institute of Biotechnology). Subsequently, qPCR was performed to determine the mRNA levels of FOXO3 and CNN3. The PCR procedure was performed as

follows: Pre-denaturation at 94°C for 5 min 10 sec, annealing at 60°C for 20 sec, extension at 72°C for 30 sec, followed with 40 cycles of 72°C for 2 min and 30 sec, 40°C for 1 min 30 sec, melting 60-94°C every 1°C for 1 sec, and 25°C for 1-2 min. The primers were synthesized by General Biology Co., Ltd., and all primer information is presented in Table II. The PCR data were analyzed using the 2^{- $\Delta\Delta\text{C}_q$} method (22).

Western blot analysis. Protein was extracted from the DB or SU-DHL-4 cells using RIPA lysis buffer (Beijing Solarbio Science & Technology Co., Ltd.) supplemented with 1% phenylmethylsulfonyl fluoride (Beijing Solarbio Science & Technology Co., Ltd.). The protein concentration was determined using a BCA protein assay kit (Beijing Solarbio Science & Technology Co., Ltd.). After mixing with 6X loading buffer, the protein was denatured in boiling. A total of 20 μl of protein sample (10-20 μg protein) was loaded onto sodium lauryl sulfate-polyacrylamide gel, and subjected to electrophoresis. The gel concentration was 5-12% depending on the protein size. Subsequently, the proteins were transferred onto PVDF membranes, blocked with skim milk (Sangon Biotech Co., Ltd.) at room temperature for 30 min, and incubated with the following antibodies at a 1:1,000 dilution at 4°C overnight: Rabbit proliferation cell nuclear antigen (PCNA; cat. no. 24036-1-AP; Wuhan Sanying Biotechnology), rabbit cyclin D1 (cat. no. AF0931; Affinity Biosciences), rabbit cyclin-dependent kinase (CDK)6 (cat. no. A0106, ABclonal Biotech Co., Ltd.), rabbit CDK2 (cat. no. A0294; ABclonal Biotech Co., Ltd.), rabbit phosphorylated retinoblastoma transcription co-repressor (pRB; Ser807/811; cat. no. AP0484; ABclonal Biotech Co., Ltd.), rabbit cleaved caspase-3 (cat. no. AF7022, Affinity Biosciences), rabbit cleaved poly ADP-ribose polymerase-1 (PARP-1; cat. no. AF7023, ABclonal Biotech Co., Ltd.), cleaved caspase-9 (cat. no. 20750; Cell Signaling Technology, Inc.), rabbit FOXO3 (cat. no. A0102; ABclonal Biotech Co., Ltd.), rabbit CNN3 (cat. no. DF9323; Affinity Biosciences) or mouse GAPDH (cat. no. 60004-1-Ig; Wuhan Sanying Biotechnology). After rinsing with 0.15% TBST buffer, the protein was incubated with goat anti-rabbit IgG labeled with horseradish peroxidase (HRP; cat. no. SE134; Beijing Solarbio Science & Technology Co., Ltd.) or goat anti-mouse IgG labeled with HRP (cat. no. SE131; Beijing Solarbio Science & Technology Co., Ltd.) at a 1:3,000 dilution, and reacted with ECL reagent (Beijing Solarbio Science & Technology Co., Ltd.), followed by signal exposure in the dark. The optical density of the bands was analyzed using Gel-Pro-Analyzer 4.0 software (Media Cybernetics, Inc.).

Cell counting kit (CCK)-8 assay. The DB or SU-DHL-4 cells were cultured in 96-well plates. Following culture for 0 h, 24 h, 48 h or 72 h, the CCK-8 reagent (Biosharp Life Sciences) was added with 10 μl per well to treat the cells at 37°C. After 2 h later, the optical density was measured at 450 nm (OD450) of the supernatant with a microplate reader (BioTek Instruments, Inc.).

EdU assay. The DB or SU-DHL-4 cells were stained with 10 μM EdU reagent (Nanjing KeyGen Biotech. Co., Ltd.) at 37°C for 2 h, and fixed with 4% paraformaldehyde for 15 min. Subsequently, all cells were washed with PBS containing

Table I. Sequence information of siRNAs and shRNAs.

Name	Sequence (5'-3')
CNN3 siRNA-a sense	GCAAGUAUAUGAUCCCAAATT
CNN3 siRNA-a anti-sense	UUUGGGAUCAUAUACUUGCTT
CNN3 siRNA-b sense	GCUCAGUGAAGAAGGUCAATT
CNN3 siRNA-b anti-sense	UUGACCUUCUUCACUGAGCTT
CNN3 siRNA-c sense	GGAGUUAAGUAUGCAGAAATT
CNN3 siRNA-c anti-sense	UUUCUGCAUACUUAACUCCTT
CNN3 siRNA-d sense	CGGCCGAAGUCAAGAACAATT
CNN3 siRNA-d anti-sense	UUGUUCUUGACUUCGGCCGTT
siRNA NC sense	UUCUCCGAACGUGUCACGUTT
siRNA NC anti-sense	ACGUGACACGUUCGGAGAATT
CNN3 shRNA-1	GGCAAGTATATGATCCCAAATTCAAGAGATTTGGGATCATATACTTGCTTTTT
CNN3 shRNA-2	GGCTCAGTGAAGAAGGTCAATTCAAGAGATTGACCTTCTTCACTGAGCTTTTT
shRNA NC	GTTCTCCGAACGTGTCACGTTTCAAGAGAACGTGACACGTTCGGAGAATTTTT

CNN3, calponin 3; NC, normal control.

Table II. PCR primer sequences.

Gene ID	Name	Temperature (°C)	Sequence	Length of amplification (bp)
NM_001455.4	FOXO3 forward	52.9	5'-TGACGACAGTCCCTCCC-3'	112
	FOXO3 reverse	53.2	5'-GCTGGCGTTAGAATTGGT-3'	
NM_001839.5	CNN3 forward	46.4	5'-ATCATCCTCTGCGAACT-3'	136
	CNN3 reverse	45.2	5'-CCATAAGCCTGAATAGC-3'	
	ChIP CNN3 forward-1	44.4	5'-AAATCCTGCACTCCTTA-3'	138
	ChIP CNN3 reverse-1	44.1	5'-CTGACTGCTCCTGTTGT-3'	
	ChIP CNN3 forward-2	46.8	5'-ACGGTTCAACTATGATGTT-3'	166
	ChIP CNN3 reverse-2	47.6	5'-CTCTTGCCACCACTTTC-3'	

FOXO3, forkhead box O3; CNN3, calponin 3.

3% bovine serum albumin (BSA), incubated with 0.5% Triton X-100 for 20 min and incubated with Click-iT reagent (Nanjing KeyGen Biotech. Co., Ltd.) at room temperature for 30 min in the dark. Finally, the cells were stained with DAPI reagent (Beijing Solarbio Science & Technology Co., Ltd.) at room temperature for 5 min, and photographed at a x400 magnification.

Flow cytometry. Flow cytometry was conducted in order to analyze cell cycle and apoptosis of DB and SU-DHL-4 cells. For apoptosis determination, the cells were incubated with Annexin V-FITC (cat. no. BL110A, Biosharp Life Sciences) for 10 min and propidium iodide (PI) (cat. no. BL110A, Biosharp Life Sciences) for 5 min at room temperature in the dark. Subsequently, the Annexin V⁺PI⁻ cells were counted as early apoptotic cells, and Annexin V⁺PI⁺ cells were counted as late apoptotic cells. For cell cycle analysis, the cells were fixed with 70% ethanol at 4°C for 2 h, stained with PI at 37°C for 30 min in the dark, and detected using a flow cytometer (ACEA

Bioscience, Inc.). The apoptosis analysis were performed with NovoExpress 1.4.1 software (ACEA Bioscience, Inc.).

Dual-luciferase reporter assay. In order to confirm the binding between FOXO3 and the promoter sequence of CNN3, dual-luciferase reporter assay was executed in 293T cells. The cells were transfected with pGL3 vector (Shaanxi Youbio Technology Co., Ltd.) containing CNN3 promoter fragment and FOXO3 overexpression plasmid (Shaanxi Youbio Technology Co., Ltd.) at 37°C in the presence of Lipo8000 reagent (Beyotime Institute of Biotechnology) for 4-6 h. Following transfection for 48 h, the cells were collected and treated with a dual-luciferase reporter assay kit (Nanjing KeyGen Biotech. Co., Ltd.), and the Firefly and *Renilla* value was determined using a microplate reader (BioTek Instruments, Inc.).

Chromatin immunoprecipitation (ChIP). The ChIP assay was performed to confirm the binding between FOXO3 and the promoter sequence of CNN3 using a ChIP kit (cat. no. P2078,

Beyotime Institute of Biotechnology) according to the manufacturer's instruction. Briefly, the cells were transfected with FOXO3 overexpression plasmid (FOXO3 coding sequence cloned into pcDNA3.1 vector) (Shaanxi Youbio Technology Co., Ltd.). After 24 h, the cells were treated with 1% formaldehyde for crosslinking for 10 min, and terminated with adding of glycine (0.125 M). Following ultrasonication at 300 W for 10 sec for 12 times using an ultrasonic homogenizer (Ningbo Scientz Biotechnology Co., Ltd.) and centrifugation at 10,000 x g at 4°C for 20 min, the supernatant was isolated. Cell lysates (100 μ l) were added into 900 μ l dilution buffer, and incubated with agarose beads (60 μ l Protein A/G per 1 ml reaction solution) bound with antibody (IgG, cat. no. A7016, Beyotime Institute of Biotechnology; anti-FOXO3, cat. no. NBP2-16521, Novus Biologicals, LLC) at 4°C for ~2 h. Thereafter, the DNA-protein complex was eluted from beads with centrifugation at room temperature at 1,000 x g for 1 min twice, and the combination was broken by de-crosslinking in NaCl solution at 65°C overnight. The protein was degraded with proteinase K (cat. no. ST535, Beyotime Institute of Biotechnology), and the DNA was collected for PCR and electrophoresis to detect the promoter sequence of CNN3. Primer sequences are presented in Table II. The cell lysate before the incubation with beads served as input control.

Xenograft model. A total of 30 healthy BALB/C nude mice (4-6 weeks old, weighing 20-22 g) were kept in a sterile environment (12/12 h light/dark cycle at 22±1°C with a humidity of 45-55%) with free access to water and food. The mice were randomly divided into five groups as follows: The vector, CNN3, shNC, shCNN3-1 and shCNN3-2 groups (n=6 per group). The DB cells stably overexpressing CNN3 or cells in which CNN3 was silenced were mixed with an equal volume of Matrigel (Corning, Inc.), and subcutaneously injected into mice (10⁶ cells per mouse), following anesthetization with inhalant of 2-3% isoflurane (3% for induction and 2% for maintenance). At 1 week post-inoculation, the tumor volume was determined every 3 days. The maximum allowable tumor size was 15 mm. Following inoculation for 22 days, the diameter of the maximum tumor was >14 mm. Therefore, the mice underwent euthanasia with an intraperitoneal injection of pentobarbital sodium (200 mg/kg), and the subcutaneous tumors were isolated for detections. The total duration of the xenograft experiment was 22 days. The humane endpoints were set according to Institutional Animal Care and Use Committee Guidebook, and no animal was euthanized due to humane endpoint prior to the experimental endpoint. Animal death was verified by the disappearance of a heartbeat. The health and behaviors of animals were monitored daily.

The project design experimental procedure was in line with the Guide for the Care and Use of Laboratory Animals (8th Edition, NIH), and approved by the Ethics Committee of Shenyang Medical College (approval no. SYYXY2021080101).

Hematoxylin and eosin (H&E) staining. The tumor tissues were fixed with 4% paraformaldehyde at room temperature overnight, washed with non-sterile water, and dehydrated with ethanol and xylene. The tissues were then embedded with paraffin, and cut into 5- μ m-thick sections, which were deparaffinized. Subsequently, the sections were stained with

hematoxylin (Beijing Solarbio Science & Technology Co., Ltd.) for 5 min, soaked in 1% hydrochloric acid/ethanol for 3 sec, and counterstained with eosin (Sangon Biotech Co., Ltd.) for 3 min. The aforementioned incubations were performed at room temperature. Finally, the sections were re-dehydrated, and mounted with gum. Images were obtained using a photon microscope (Olympus Corporation) at a x400 magnification.

Immunohistochemical staining. The subcutaneous tumor tissues from mice were fixed into paraffin sections, as described above. Following deparaffinization, the sections reacted with antigen retrieval reagent (containing 1.8 mM citric acid and 8.2 mM sodium citrate) for 10 min. The sections were then blocked with 3% H₂O₂ and 1% BSA respectively, and incubated with antibody against PCNA (cat. no. 24036-1-AP, Wuhan Sanying Biotechnology) or cyclin D1 (cat. no. AF0931, Jiangsu Affinity Biosciences Biology Research Company) at a 1:100 dilution at 4°C overnight in a humid box. After washing with PBS, the sections were incubated with HRP-labeled IgG (cat. no. 31460, Thermo Fisher Scientific, Inc.) at a 1:500 dilution at 37°C for 60 min, reacted with DAB reagent for several seconds, and stained with hematoxylin (Beijing Solarbio Science & Technology Co., Ltd.) at room temperature for 3 min. Finally, the sections were dehydrated with ethanol and xylene (75% ethanol for 2 min, 85% ethanol for 2 min, 95% ethanol for 2 min, 100% ethanol for 5 min twice, xylene for 10 min twice), and mounted with gum. Images were obtained using a photon microscope (Olympus Corporation) at x400 magnification.

Bioinformatics analysis. The medical bank Gene Expression Profiling Interactive Analysis (GEPIA) (<http://gepia.cancer-pku.cn/>) [the dataset sources were The Cancer Genome Atlas (TCGA) and GTEx] was used to analyze the expression of CNN3 in DLBCL tissues. The expression pattern of CNN3 was analyzed by ggplot2 and circlize software, and GO enrichment analysis was carried out with clusterProfiler software. An unpaired t-test was used to compare the data between two groups. The online bioinformatics website JASPAR (<https://jaspar.genereg.net/>) was used to predict the binding between FOXO3 and promoter sequence of CNN3, and the potential binding sites were identified.

Statistical analysis. The data in the present study are presented as the mean \pm SD, and analyzed by GraphPad Prism 7.0 software (GraphPad Software, Inc.). The data from two independent groups were compared using an unpaired Student's t-test. The data from multiple groups were analyzed using one- or two-way ANOVA, followed by post hoc Bonferroni comparisons. A value of P<0.05 was considered to indicate a statistically significant difference.

Results

CNN3 is highly expressed in DLBCL specimens. The dysregulated genes in DLBCL specimens from a cancer databank GEPIA (23). Gene Expression Profiling Interactive with values P<0.001 and log₂FC>3 or <-3 were analyzed. According to Fig. 1A, 1,440 genes were highly expressed, and 206 genes were expressed at low levels in DLBCL specimens, as compared with the blood samples from healthy controls.

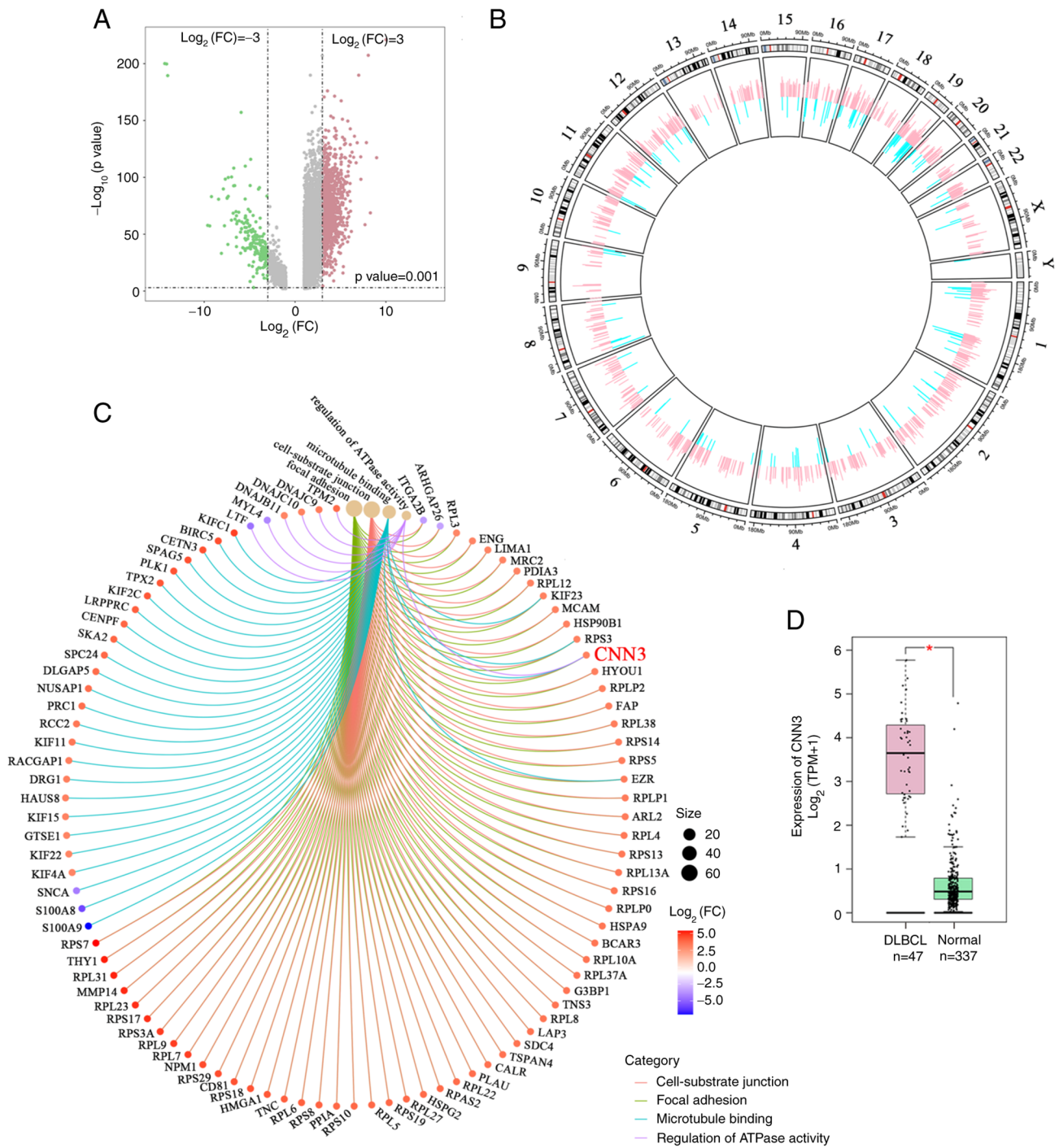


Figure 1. CNN3 is upregulated in DLBCL specimens. (A) The volcano plot illustrates the dysregulated genes in DLBCL specimens and normal blood specimens from the GEPIA databank (the dataset sources were TCGA and GTEx) using P-values and fold change values. (B) Circos plot reveals the locations of the dysregulated genes on chromosomes. (C) GO enrichment analysis displays the expression pattern of genes with abnormal expression. (D) The analysis of CNN3 mRNA expression in DLBCL specimens. CNN3, calponin 3; DLBCL, diffuse large B-cell lymphoma; GEPIA, Gene Expression Profiling Interactive Analysis; TCGA, The Cancer Genome Atlas; GO, Gene Ontology.

These abnormally expressed genes were distributed in all chromosomes (Fig. 1B). Gene Ontology (GO) enrichment analysis revealed that CNN3 was simultaneously enriched in four pathways, namely focal adhesion, cell-substrate junction, microtubule binding, and the regulation of ATPase activity in DLBCL specimens (Fig. 1C). An additional analysis revealed that CNN3 mRNA expression was significantly upregulated in DLBCL specimens, as compared with normal blood samples (Fig. 1D).

CNN3 promotes the proliferation and cell cycle transition of DLBCL cells. The overexpression vector and siRNAs targeting CNN3 were synthesized and transfected into DB and SU-DHL-4 cells in order to regulate the expression of CNN3, and RT-qPCR and western blot analysis confirmed the overexpression and silencing efficiency (Fig. 2). The results of CCK-8 assay revealed that the viability of CNN3-overexpressing DB and SU-DHL-4 cells was increased and that of the CNN3-silenced cells was decreased (Fig. 3A and B). Edu

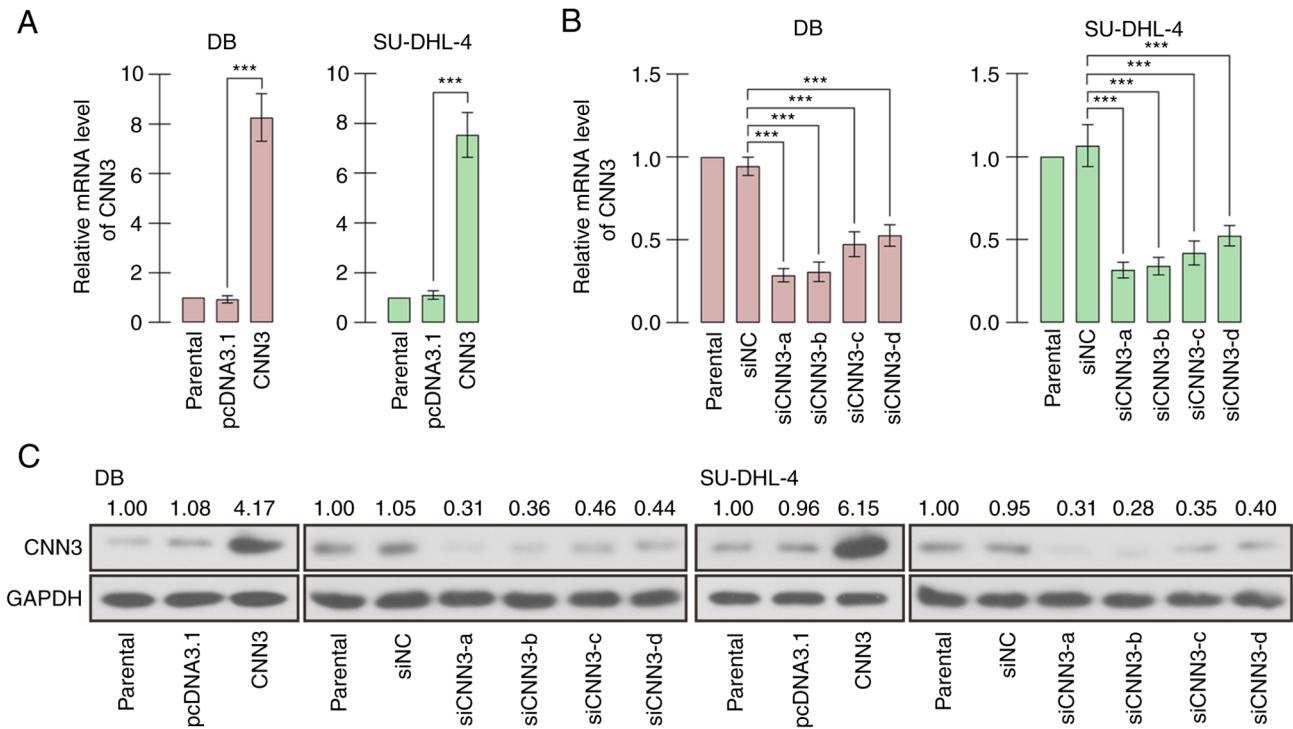


Figure 2. Overexpression and knockdown of CNN3 in DLBCL cells. The changes in the expression of CNN3 in DB and SU-DHL-4 cells were confirmed using (A and B) reverse transcription-quantitative PCR and (C) western blot analysis following transfection with CNN3 overexpression vector or siRNA. *** $P < 0.001$. CNN3, calponin 3; DLBCL, diffuse large B-cell lymphoma.

staining revealed that the live cell numbers were increased following the ectopic expression of CNN3, and decreased following CNN3 knockdown, compared with the empty vector or siNC control (Fig. 3C). Western blot analysis revealed that the expression of the proliferation marker, PCNA, was elevated following CNN3 overexpression and decreased following CNN3 silencing (Fig. 3D). Subsequently, the results of flow cytometry of the DB and SU-DHL-4 cells demonstrated that CNN3 overexpression elevated the proportion of cells in the S phase and reduced the proportion of cells in the G1 phase (Fig. 4A and B). Additionally, the proportion of cells in the S phase was decreased and that of cells in the G1 phase was increased following the knockdown of CNN3 (Fig. 4A and C). Thereafter, the expression of several cell cycle-related proteins was measured using western blot analysis. The results revealed that the levels of cyclin D1, CDK6, CDK2 and (Ser801/811) were increased following the overexpression of CNN3 and decreased following CNN3 silencing (Fig. 4D). These results suggested that CNN3 facilitated the proliferation and cell cycle G1/S transition of DLBCL cells.

CNN3 silencing induces the apoptosis of DLBCL cells. The apoptosis of the DB and SU-DHL-4 cells was analyzed using flow cytometry. As shown in Fig. 5A and B, it was evident that CNN3 knockdown significantly induced the apoptosis of the DB and SU-DHL-4 cells, including both early (Annexin V⁺PI⁻) and late apoptosis (Annexin V⁺PI⁺). The results of western blot analysis also revealed that the levels of the apoptotic markers, cleaved caspase-3/9 and cleaved PARP-1, were increased in the CNN3-silenced DB and SU-DHL-4 cells (Fig. 5C). On the whole, these results suggested that CNN3

knockdown resulted in the increased apoptosis of DLBCL cells.

CNN3 enhances the growth of DLBCL cells in vivo. A tumor xenograft experiment was carried out to detect the effects of CNN3 on the growth of DLBCL cells in nude mice. The DB cells with stably overexpressing CNN3 or cells in which CNN3 was silenced were screened, and alterations in expression were confirmed using RT-qPCR and western blot analysis (Fig. 6A and B). The screened DB cells were subcutaneously inoculated into mice for 22 days. The results demonstrated that the growth of CNN3-overexpressing DB cells was increased and that of the CNN3-silenced cells was decreased, in comparison to the growth of the respective controls (Fig. 6C-E). H&E staining revealed nuclear shrinkage and intercellular cavity in the CNN3-silenced tumors, whereas the CNN3-overexpressing tumors were more compactly structured in comparison with the control (Fig. 6F). Immunohistochemical staining revealed that the expression of PCNA and cyclin D1 was increased in tumors overexpressing CNN3, suggesting that CNN3 facilitated the growth of DB cells; by contrast, PCNA and cyclin D1 expression was decreased in tumors derived from CNN3-silenced cells, suggesting the inhibition of tumor growth (Fig. 6G).

CNN3 expression is negatively regulated by FOXO3. The analysis from bioinformatics websites demonstrated that the promoter sequence of CNN3 was potentially bound by FOXO3, and the latent binding sites are displayed in Fig. 7A. The analysis from the GEPIA database revealed that the FOXO3 expression was slightly decreased in DLBCL specimens, in

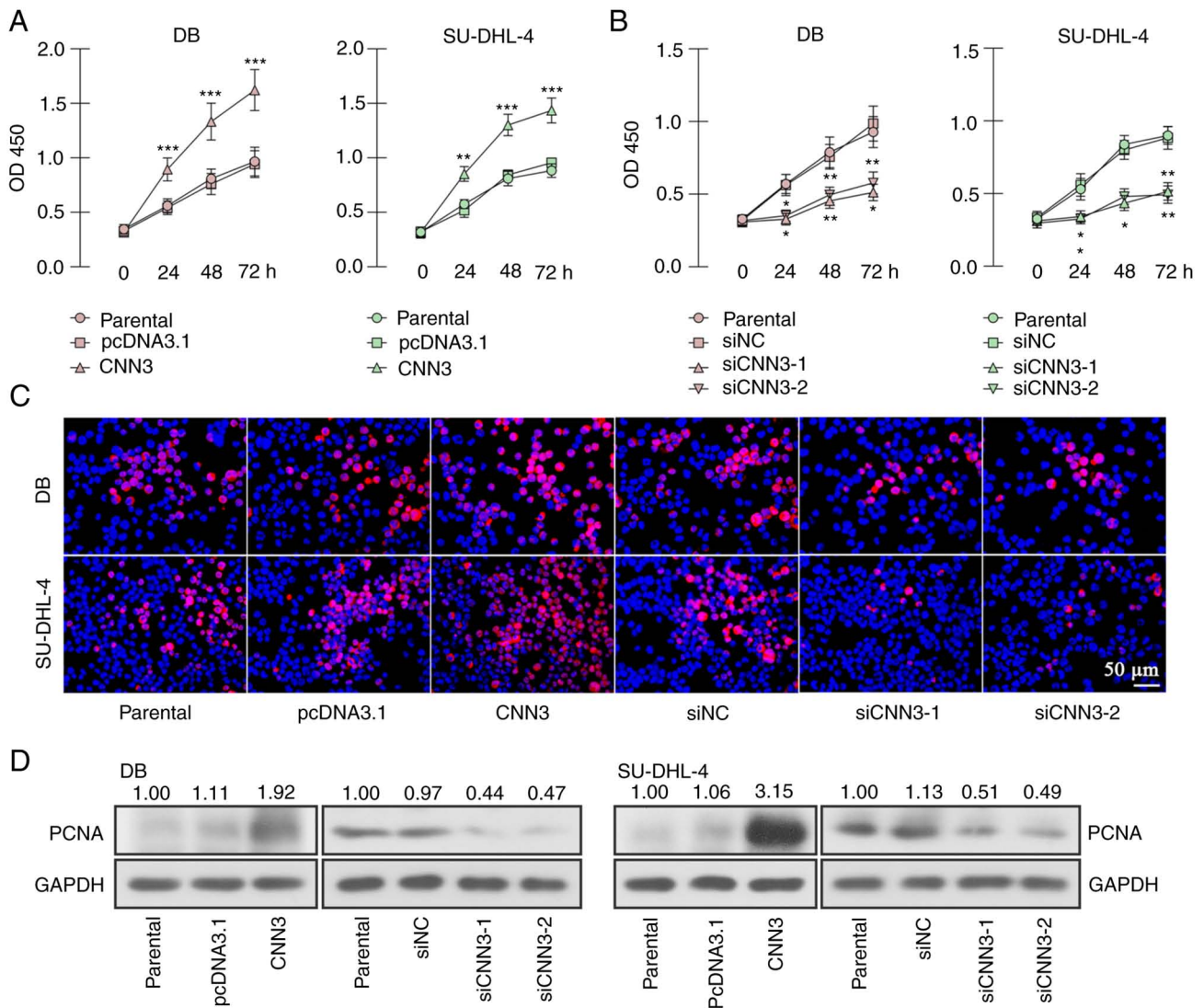


Figure 3. CNN3 promotes the proliferation of DLBCL cells. (A and B) CCK-8 assay was used to measure the viability of DB and SU-SHL-4 cells following the (A) ectopic expression or (B) knockdown of CNN3. (C) EdU staining was performed to display live cells. (D) The expression of the proliferation marker, PCNA. * $P < 0.05$, ** $P < 0.01$ and *** $P < 0.001$ vs. pcDNA3.1 or siNC group. CNN3, calponin 3; DLBCL, diffuse large B-cell lymphoma; CCK, Cell Counting Kit; PCNA, proliferation cell nuclear antigen.

comparison with normal blood samples (Fig. 7B). In order to investigate the function of FOXO3, a FOXO3 overexpression vector was constructed and its availability was verified at the transcription and translation levels in DB and SU-DHL-4 cells (Fig. 7C and D). The mRNA and protein expression levels of CNN3 were simultaneously decreased by ~50% following FOXO3 overexpression (Fig. 7E and F). Dual-luciferase reporter assay demonstrated that the suppression of FOXO3 luciferase activity of the reporter vector containing the CNN3 promoter sequence was significantly attenuated following the deletion of the -1955/-1948 and -1190/-1183 sites, particularly the former (Fig. 7G). ChIP assay revealed that FOXO3 certainly bound to the -1955/-1948 and -1190/-1183 sites of CNN3 promoter sequence. In addition, the binding affinity of FOXO3 to -1955/-1948 site appeared greater than that to the -1190/-1183 site (Fig. 7H).

Thereafter, rescue experiments were performed by the co-expression of FOXO3 and CNN3. The overexpression vector of CNN3 only contained its coding sequence, not

the promoter sequence. Thus, the ectopic expression of CNN3 was not regulated by FOXO3. As demonstrated in Fig. 8A, the transfection of the CNN3 overexpression vector reversed the FOXO3-induced decrease in CNN3 expression. Moreover, the recovered CNN3 expression abrogated the FOXO3-induced inhibition of the proliferation and cell cycle transition, and the induction of apoptosis of DB cells (Fig. 8B-F). On the whole, these results suggested that FOXO3 bound to the promoter of CNN3 and negatively regulated its tumor-promoting roles in DLBCL cells (Fig. 8G).

Discussion

FOX is an evolutionarily conserved transcription factor family, which has a deeply conserved forkhead winged helix-turn-helix DNA binding domain (24). FOXO3, also known as FOXO3a or forehead in rhabdomyosarcoma-like 1, belongs to the FOXO subfamily (25). FOXO3 mediates multiple pathological and physiological processes by

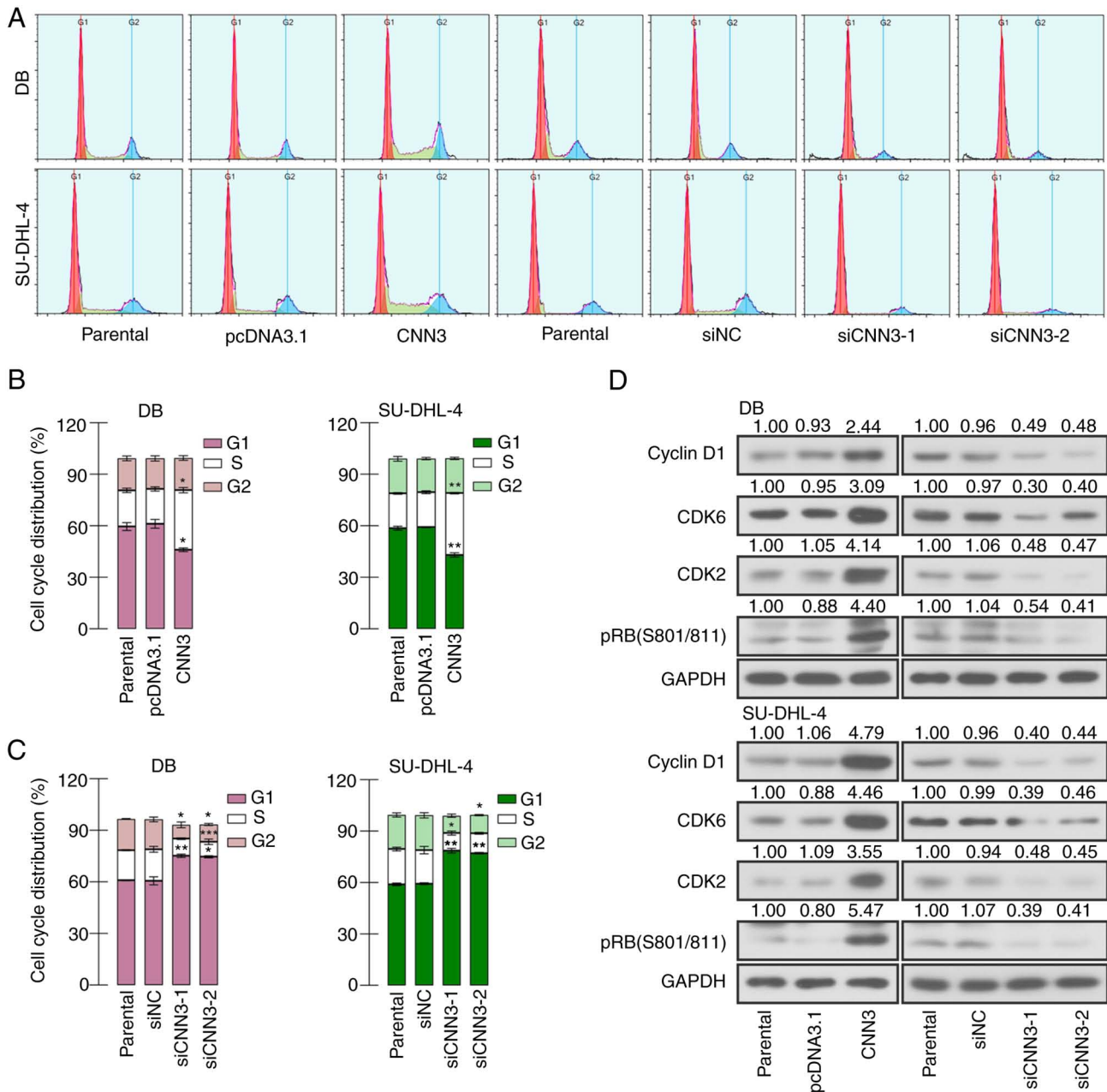


Figure 4. CNN3 accelerates the cell cycle transition of DLBCL cells. (A-C) The cell cycle distribution of DB and SU-DHL-4 cells was analyzed using flow cytometry. (D) The levels of several cell cycle-related proteins, cyclin D1, CDK6, CDK2 and pRB (S801/811) in CNN3-overexpressing or silenced cells. * $P < 0.05$, ** $P < 0.01$ and *** $P < 0.001$ vs. the pcDNA3.1 or the siNC group. CNN3, calponin 3; DLBCL, diffuse large B-cell lymphoma; CDK, cyclin-dependent kinase; pRB, phosphorylated retinoblastoma transcription co-repressor.

controlling the transcription of target genes involved in cell proliferation, cell cycle transition, apoptosis, DNA damage and autophagy (26). It has been reported that FOXO3 inhibited tumorigenesis by suppressing the expression of proliferation-related genes, including CCND1 (27) and CCNA1 (28), and inducing the expression of apoptotic genes, including BIM (29) and NOXA (30). The loss of FOXO3 expression significantly accelerates B lymphomagenesis in MYC-mutant mice (31), and the silencing of FOXO3 inhibits the apoptosis of DLBCL cells (17). In the present study, the ectopic expression of FOXO3 induced the apoptosis, and attenuated the proliferation and cell cycle transition of DLBCL cells. It was also demonstrated that FOXO3 bound to the promoter sequence of CNN3 and suppressed its

transcription, with the effects of FOXO3 being significantly reversed by CNN3 expression.

The cancer-promoting roles of CNN3 have been reported in several solid tumors, and its effect on lymphomagenesis was first demonstrated in the present study, to the best of our knowledge. CNN3 is an isoform of calponin, acting as an actin-binding protein for the inhibition of myosin ATPase and the stabilization of the actin cytoskeleton (32). CNN3 affects the motility, migration, adhesion, differentiation, phagocytosis and fusion of multiple cells by regulating the actin cytoskeleton. Its effects on proliferation have been reported in recent years. For instance, CNN3 knockdown impairs the proliferation of myoblasts and fibroblasts (33,34). Increased expression of CNN3 promoted the proliferation of

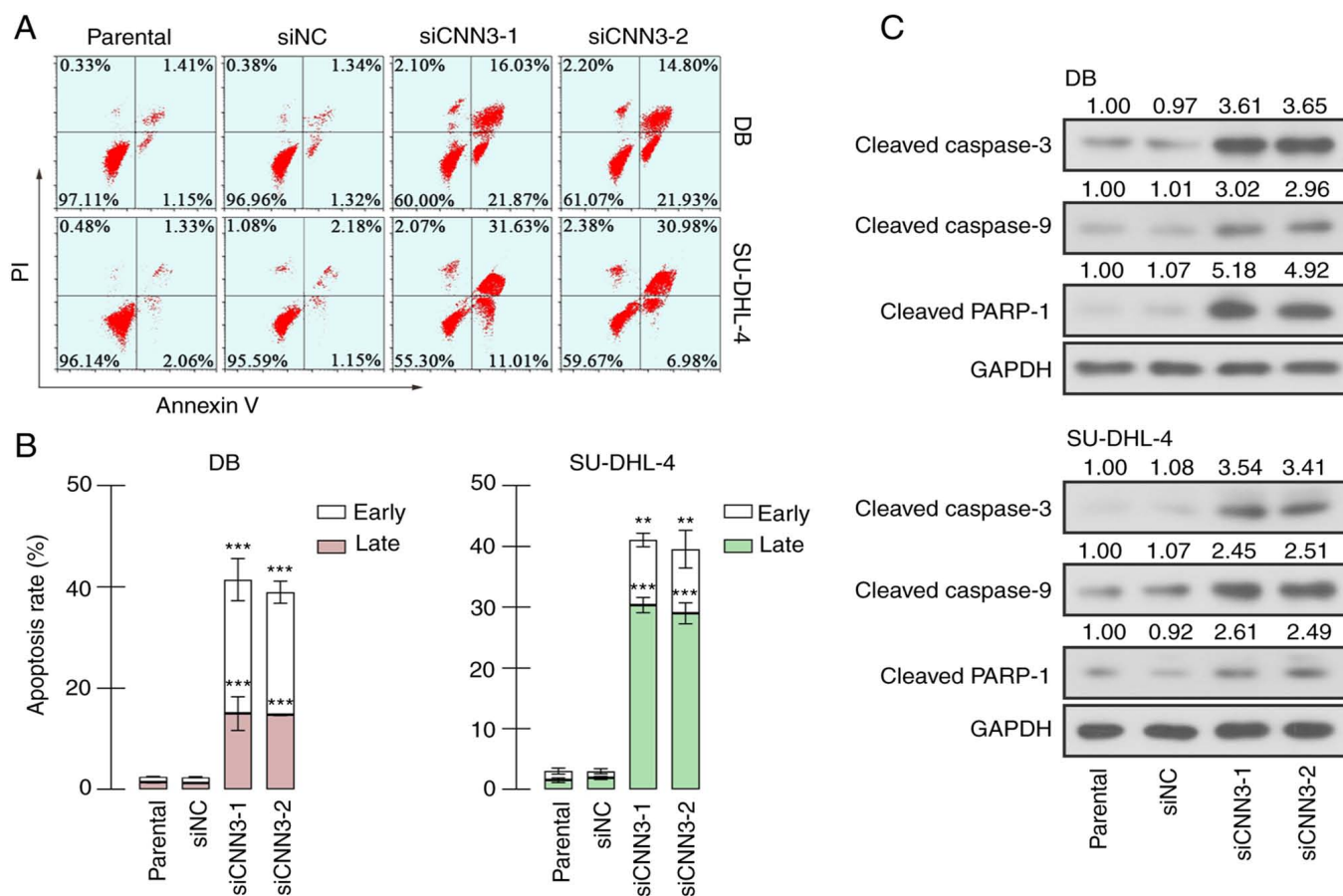


Figure 5. CNN3 silencing induces the apoptosis of DLBCL cells. (A and B) The apoptosis of DB and SU-DHL-4 cells was measured using flow cytometry with Annexin V and PI staining. Annexin V⁺PI⁻ cells were considered as early apoptotic cells, and Annexin V⁺PI⁺ cells as late apoptotic cells. (C) The levels of several apoptosis markers, cleaved caspase-3, cleaved caspase-9 and cleaved PARP-1, were examined in CNN3-silenced cells. **P<0.01 and ***P<0.001 vs. pcDNA3.1 or siNC group). CNN3, calponin 3; DLBCL, diffuse large B-cell lymphoma; PI, propidium iodide.

osteosarcoma and cervical cancer cells (11,35). By contrast, in a previous study by Yang *et al* (36), CNN3 was reported to suppress the proliferation of lung cancer cells. The tumor databank analysis demonstrated that the expression of CNN3 in tumor specimens was relatively different, compared with their respective control normal tissues, suggesting that CNN3 may be expressed with tissue specificity, resulting in its discrepant functions in different organs and tissues. Nevertheless, this speculation requires further verification in future studies. In the present study, CNN3 was highly expressed in DLBCL specimens, accompanied by promoting effects on the proliferation of DLBCL cells. However, the clinical data from the tumor databank analyzed in the present study included DLBCL specimens and normal blood samples (the dataset sources are TCGA and GTEx). It was hypothesized that it may be more reasonable to compare the expression of CNN3 in DLBCL specimens and normal lymph node tissues. Due to the difficulty of normal lymph node collection, this comparison has not yet been realized. In future studies, the authors aim to collect DLBCL specimens and normal lymph node tissues to confirm the expression of CNN3.

The data of the present study demonstrated that CNN3 promoted the proliferation and cell cycle transition, and its knockdown stimulated the apoptosis of DLBCL cells. In the majority of adult tissues, cells are in a quiescent state

(G0 phase), and can be stimulated to re-enter the cell cycle by mitogenic signals. Uncontrolled proliferation and abnormally activated cell cycle are the primary characteristics of malignant cells (37). Cyclins interact with CDKs for the regulation of the G0/G1, S, G2 and M phase progression in mammalian cells (37). Cyclin D firstly senses the mitogenic signals, binding to CDK4 and CDK6, and cells enter the G1 phase to initiate DNA synthesis (38,39). The activation of the cyclin D-CDK4/6 complex phosphorylates the pocket protein including RB to enable E2F transcription factor to induce the transcription of downstream genes involved in cell cycle. This includes cyclin E, which binds to CDK2, with the formed complex further phosphorylating RB to create a positive feedback loop (37,38,40). In the results of the present study, CNN3 induced the increased levels of cyclin D1, CDK6, CDK2 and pRB in DLBCL cells, accompanied by an accelerated G1/S transition. These data suggested that CNN3 facilitated the proliferation of DLBCL cells by accelerating cell cycle G1/S transition.

Suppressed apoptosis is another characteristic of malignant tumor cells. Apoptosis is a type of cell death actively initiated by cells themselves, and helpful for the survival of the whole organism. The apoptotic process in mammalian cells is evolutionarily conserved and precisely regulated. The extrinsic apoptotic signals are delivered by death receptors,

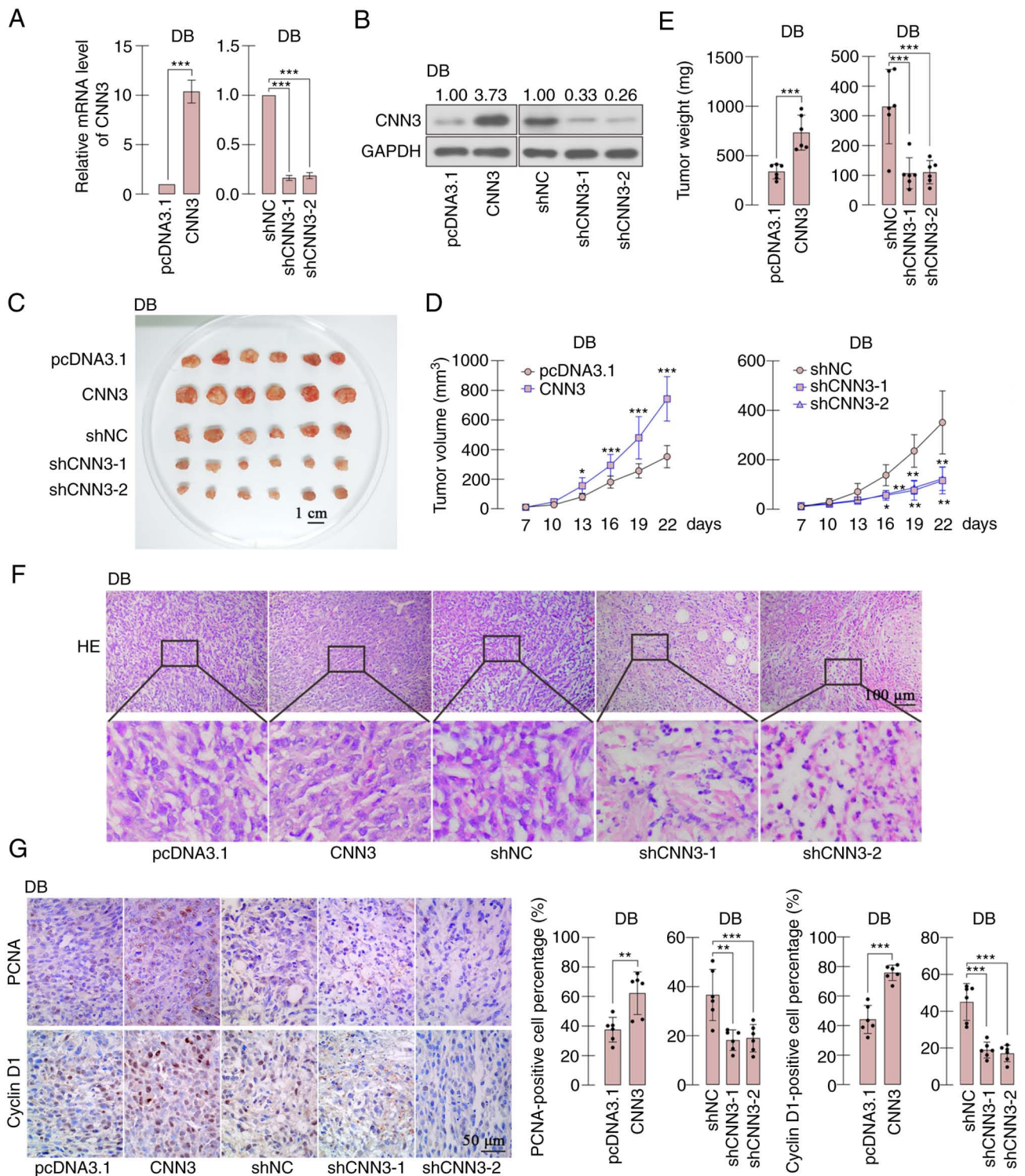


Figure 6. CNN3 enhances growth of DLBCL cells *in vivo*. (A) reverse transcription-quantitative PCR and (B) western blot analysis were used to confirm the effectiveness of the stable overexpression or knockdown of CNN3 in DB cells. (C) Subcutaneous tumors formed by DB cells with varying expression levels of CNN3 (scale bar corresponds to 1 cm). (D) The growth curve of tumors. (E) Tumor weight. (F) H&E staining was performed to detect the pathological alteration in tumors (the scale bar corresponds to 100 μm). (G) The expression of PCNA and cyclin D1 in tumors was examined using immunohistochemical staining and quantitatively analyzed (scale bar corresponds to 50 μm). * $P < 0.05$, ** $P < 0.01$ and *** $P < 0.001$ vs. pcDNA3.1 or shNC group. CNN3, calponin 3; DLBCL, diffuse large B-cell lymphoma; NC, normal control; H&E, hematoxylin and eosin.

including Fas and tumor necrosis factor receptors (TNFRs), and their adapters, including Fas-associated death domain and TNFR-associated death domain to active caspase-8 (41,42). Intrinsic apoptosis is initiated by the mitochondrial pathway. The permeability of the mitochondrial membrane is increased

and cytochrome *c* is released into the cytoplasm to activate caspase-9 (43). The intrinsic and extrinsic apoptotic pathways merge to caspase-3, a well-known executioner agent that is responsible for the cleavage of protein kinase, DNA repair proteins and cytoskeletal proteins (44). PARPs are

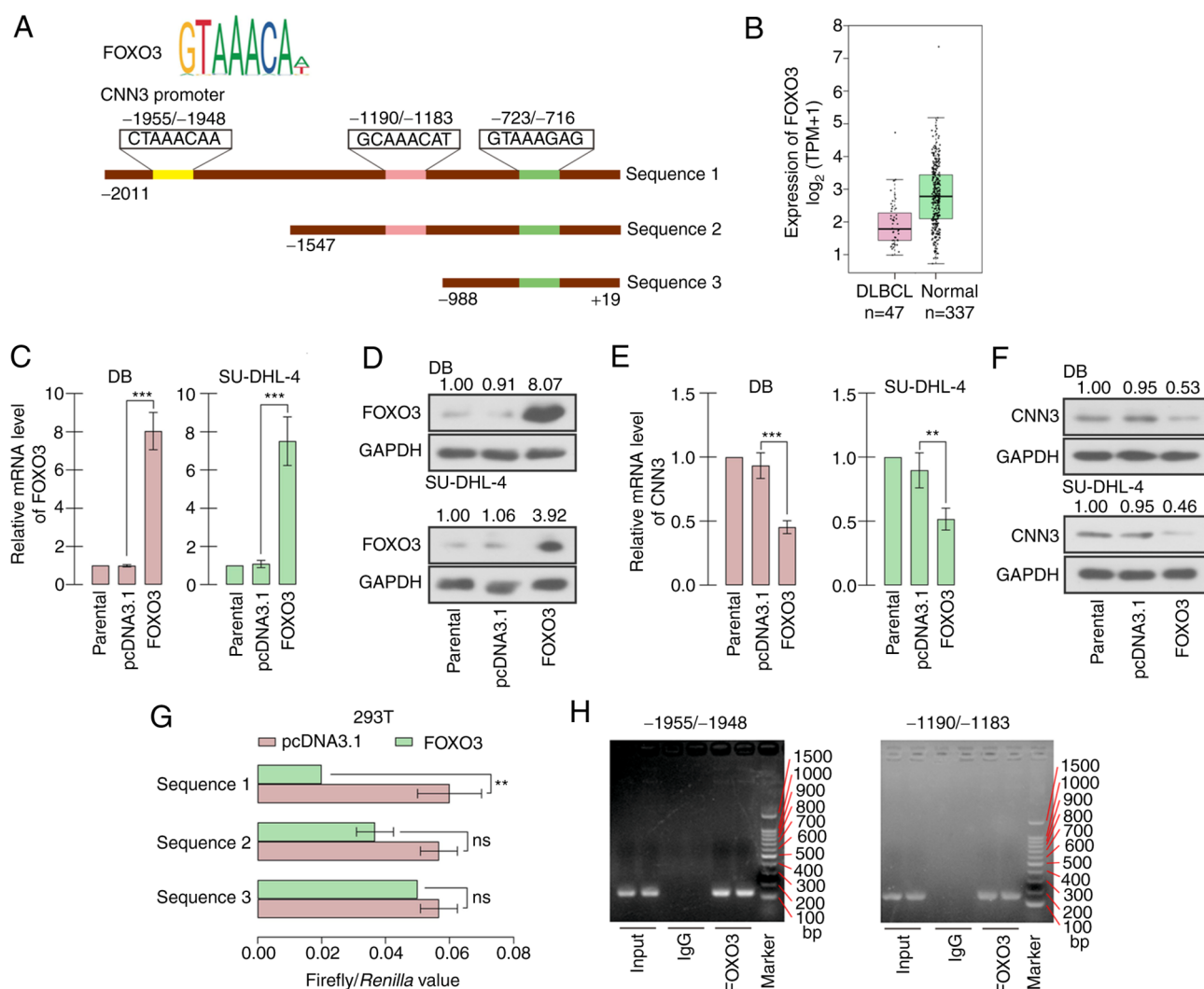


Figure 7. CNN3 expression is negatively regulated by FOXO3. (A) The conserved binding sequence of FOXO3, and the three potential binding sites in CNN3 promoter are illustrated. (B) FOXO3 expression in DLBCL specimens and normal blood samples from the GEPIA databank. (C and D) The efficacy of FOXO3 overexpression was confirmed in DB and SU-DHL-4 cells. (E and F) CNN3 expression was examined using (E) reverse transcription-quantitative PCR and (F) western blot analysis following the induction of enhanced FOXO3 expression. (G) Dual-luciferase reporter assay was carried out to verify the binding between FOXO3 and CNN3 promoter sequence in 293T cells. (H) ChIP assay was used to confirm the binding between FOXO3 and -1955/-1948 or -1190/-1183 site in CNN3 promoter sequence. ** $P < 0.01$ and *** $P < 0.001$ vs. the pcDNA3.1 group. CNN3, calponin 3; FOXO3, forkhead box O3; DLBCL, diffuse large B-cell lymphoma; GEPIA, Gene Expression Profiling Interactive Analysis.

poly-ADP-ribosyltransferases that mediate poly-ADP-ribosylation of nuclear proteins involved in DNA repair. Among 18 members of the PARP subfamily, PARP-1 has been the most extensively studied (45). PARP-1 catalyzes the synthesis of polymers of ADP-ribose with NAD^+ as substrates (46). In response to DNA strand breakage, PARP-1 is cleaved and activated by caspase-3 (47); thus, the presence of cleaved PARP-1 is generally considered as a marker of apoptosis (46). In the present study, the levels of cleaved caspase-3, caspase-9 and PARP-1 were all increased following CNN3 knockdown, suggesting the activation of the intrinsic apoptosis of DLBCL cells. Moreover, flow cytometry was used to measure the apoptosis by Annexin V and PI staining. In the early stage of apoptosis, the phosphatidylserine (PS) in the inner layers of cytomembrane is flipped out to the outer layers to be recognized for phagocytosis (41). As a phospholipid binding protein, Annexin V specifically and strongly interacts with PS, and the labeled Annexin V can indicate early apoptotic cells (48). In

the middle and late stages of apoptosis, PI can pass through the impaired cytomembrane to stain DNA; thus, Annexin V⁺PI⁺ is considered as a marker of late apoptosis. The present study also demonstrated that CNN3 silencing concurrently triggered the early and late apoptosis of DLBCL cells.

DLBCL is a malignant tumor originating from lymphoid tissue. Due to its high heterogeneity, there are variations in the treatment and outcomes of patients with DLBCL. Based on gene expression profiling, DLBCL is divided into two distant subtypes: Germinal center B-cell-like (GCB) and activated B-cell-like (ABC). These two subtypes arise from different stages of lymphoid differentiation with separate oncogenic mechanisms, and the prognosis of patients with the ABC subtype is poorer (49-51). For instance, B-cell receptor signaling and nuclear factor κB are generally activated in the ABC subtype and B-cell leukemia/lymphoma 6 and enhancer of zeste 2 polycomb repressive complex 2 subunit tend to be expressed in the GCB subtype (52). Both FOXO3 and CNN3

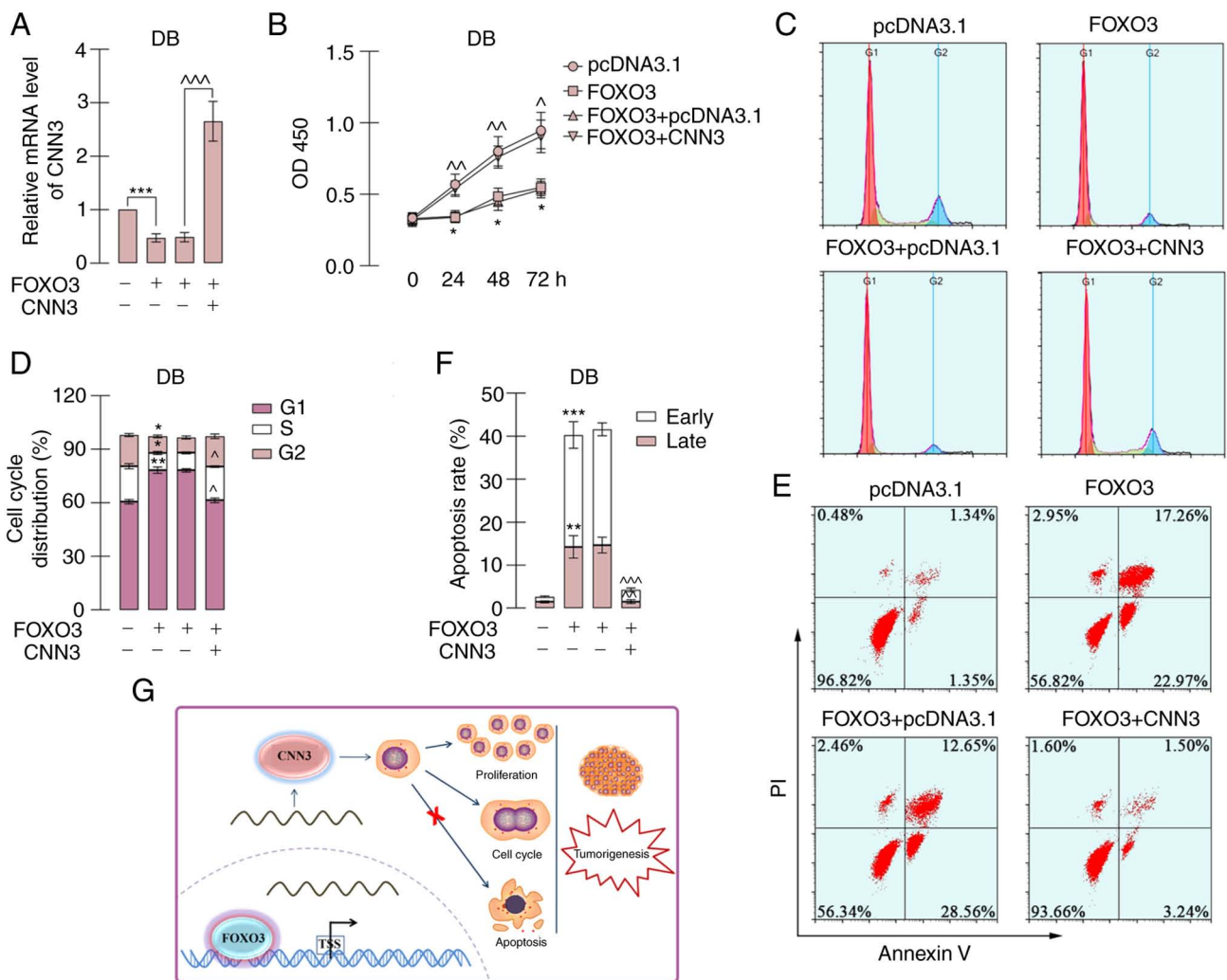


Figure 8. Effects of FOXO3 on DLBCL cells were abolished by CNN3. (A) The mRNA level of CNN3 in DB cells. (B) Cell viability was detected using CCK-8 assay. (C and D) Cell cycle distribution was analyzed using flow cytometry. (E and F) Apoptotic levels were measured using flow cytometry with Annexin V and PI staining. (G) FOXO3-regulated CNN3 promoted the tumorigenesis of DLBCL cells by enhancing proliferation and cell cycle transition, and suppressing apoptosis. * $P < 0.05$, ** $P < 0.01$ and *** $P < 0.001$ vs. the pcDNA3.1 group; $^{\wedge}P < 0.05$, $^{\wedge\wedge}P < 0.01$ and $^{\wedge\wedge\wedge}P < 0.001$ vs. the FOXO3+pcDNA3.1 group. FOXO3, forkhead box O3; DLBCL, diffuse large B-cell lymphoma; CNN3, calponin 3; CCK-8, Cell Counting Kit-8; PI, propidium iodide.

have not been found to be associated with the classification of DLBCL. The authors aim to investigate the outcomes of patients with DLBCL with a high or low expression of FOXO3 or CNN3 and the association between FOXO3 or CNN3 and the ABC/GCB subtype in future studies. Nevertheless, the findings of the present study suggested that FOXO3 and CNN3 may be considered as novel therapeutic targets for DLBCL.

In conclusion, the present study demonstrated that CNN3 promoted tumor growth *in vivo* and *in vitro*, and cell cycle G1/S transition, and inhibited the apoptosis of DLBCL cells. FOXO3 bound the promoter sequence of CNN3 and inhibited its transcription. The lymphoma suppressive roles of FOXO3 were antagonized by CNN3 overexpression. These findings may provide novel insight into the diagnosis and treatment of patients with DLBCL in clinical practice.

Acknowledgements

Not applicable.

Funding

The present study was supported by the National Natural Science Foundation of China (grant no. U1908215), the General Program of the National Natural Science Foundation of China (grant no. 62273330), and the Fundamental Research Funds for the Central Universities, the Provincial and Ministerial Science Foundation (Millions of Talents Project of Liaoning Province in 2019).

Availability of data and materials

The datasets used and/or analyzed during the current study are available from the corresponding author on reasonable request.

Authors' contributions

XX designed the study and coordinated the experiments. ML, XW, QG and HW performed the experiments and analyzed the data. The manuscript was drafted by XX. All authors have

read and approved the final manuscript. XX and ML confirmed the authenticity of all the raw data.

Ethics approval and consent to participate

The project design experimental procedure was in line with Guide for the Care and Use of Laboratory Animals (8th Edition, NIH), and approved by the Ethics Committee of Shenyang Medical College (approval no. SYYXY2021080101).

Patient consent for publication

Not applicable.

Competing interests

The authors declare that they have no competing interests.

References

- Armitage JO, Gascoyne RD, Lunning MA and Cavalli F: Non-Hodgkin lymphoma. *Lancet* 390: 298-310, 2017.
- Guerard EJ and Bishop MR: Overview of non-Hodgkin's lymphoma. *Dis Mon* 58: 208-218, 2012.
- Martelli M, Ferreri AJ, Agostinelli C, DiRocco A, Pfreundschuh M and Pileri SA: Diffuse large B-cell lymphoma. *Crit Rev Oncol Hematol* 87: 146-171, 2013.
- Liu Y and Barta SK: Diffuse large B-cell lymphoma: 2019 Update on diagnosis, risk stratification, and treatment. *Am J Hematol* 94: 604-616, 2019.
- Winder SJ and Walsh MP: Smooth muscle calponin. Inhibition of actomyosin MgATPase and regulation by phosphorylation. *J Biol Chem* 265: 10148-10155, 1990.
- Winder SJ, Walsh MP, Vasulka C and Johnson JD: Calponin-calmodulin interaction: Properties and effects on smooth and skeletal muscle actin binding and actomyosin ATPases. *Biochemistry* 32: 13327-13333, 1993.
- Kake T, Kimura S, Takahashi K and Maruyama K: Calponin induces actin polymerization at low ionic strength and inhibits depolymerization of actin filaments. *Biochem J* 312: 587-592, 1995.
- Ferhat L, Esclapez M, Represa A, Fattoum A, Shirao T and Ben-Ari Y: Increased levels of acidic calponin during dendritic spine plasticity after pilocarpine-induced seizures. *Hippocampus* 13: 845-858, 2003.
- Flemming A, Huang QQ, Jin JP, Jumaa H and Herzog S: A conditional knockout mouse model reveals that calponin-3 is dispensable for early B cell development. *PLoS One* 10: e0128385, 2015.
- Shibukawa Y, Yamazaki N, Kumasawa K, Daimon E, Tajiri M, Okada Y, Ikawa M and Wada Y: Calponin 3 regulates actin cytoskeleton rearrangement in trophoblastic cell fusion. *Mol Biol Cell* 21: 3973-3984, 2010.
- Xia L, Yue Y, Li M, Zhang YN, Zhao L, Lu W, Wang X and Xie X: CNN3 acts as a potential oncogene in cervical cancer by affecting RPLP1 mRNA expression. *Sci Rep* 10: 2427, 2020.
- Nair VA, Al-Khayyal NA, Sivaperumal S and Abdel-Rahman WM: Calponin 3 promotes invasion and drug resistance of colon cancer cells. *World J Gastrointest Oncol* 11: 971-982, 2019.
- Hong KS, Kim H, Kim SH, Kim M and Yoo J: Calponin 3 regulates cell invasion and doxorubicin resistance in gastric cancer. *Gastroenterol Res Pract* 2019: 3024970, 2019.
- Tsuji T, Maeda Y, Kita K, Murakami K, Saya H, Takemura H, Inaki N, Oshima M and Oshima H: FOXO3 is a latent tumor suppressor for FOXO3-positive and cytoplasmic-type gastric cancer cells. *Oncogene* 40: 3072-3086, 2021.
- Shukla S, Bhaskaran N, MacLennan GT and Gupta S: Deregulation of FoxO3a accelerates prostate cancer progression in TRAMP mice. *Prostate* 73: 1507-1517, 2013.
- Blake DC Jr, Mikse OR, Freeman WM and Herzog CR: FOXO3a elicits a pro-apoptotic transcription program and cellular response to human lung carcinogen nicotine-derived nitrosamino-ketone (NNK). *Lung Cancer* 67: 37-47, 2010.
- Zheng X, Rui H, Liu Y and Dong J: Proliferation and apoptosis of B-cell lymphoma cells under targeted regulation of FOXO3 by miR-155. *Mediterr J Hematol Infect Dis* 12: e2020073, 2020.
- Bi C and Wang G: LINC00472 suppressed by ZEB1 regulates the miR-23a-3p/FOXO3/BID axis to inhibit the progression of pancreatic cancer. *J Cell Mol Med* 25: 8312-8328, 2021.
- Yu S, Yu Y, Zhang W, Yuan W, Zhao N, Li Q, Cui Y, Wang Y, Li W, Sun Y and Liu T: FOXO3a promotes gastric cancer cell migration and invasion through the induction of cathepsin L. *Oncotarget* 7: 34773-34784, 2016.
- Hu C, Ni Z, Li BS, Yong X, Yang X, Zhang JW, Zhang D, Qin Y, Jie MM, Dong H, *et al*: hTERT promotes the invasion of gastric cancer cells by enhancing FOXO3a ubiquitination and subsequent ITGB1 upregulation. *Gut* 66: 31-42, 2017.
- Bouzeyen R, Haoues M, Barbouche MR, Singh R and Essafi M: FOXO3 transcription factor regulates IL-10 expression in mycobacteria-infected macrophages, tuning their polarization and the subsequent adaptive immune response. *Front Immunol* 10: 2922, 2019.
- Livak KJ and Schmittgen TD: Analysis of relative gene expression data using real-time quantitative PCR and the 2(-Delta Delta C(T)) method. *Methods* 25: 402-408, 2001.
- Tang Z, Li C, Kang B, Gao G, Li C and Zhang Z: GEPIA: A web server for cancer and normal gene expression profiling and interactive analyses. *Nucleic Acids Res* 45: W98-W102, 2017.
- Benayoun BA, Caburet S and Veitia RA: Forkhead transcription factors: Key players in health and disease. *Trends Genet* 27: 224-232, 2011.
- Anderson MJ, Viars CS, Czekay S, Cavenee WK and Arden KC: Cloning and characterization of three human forkhead genes that comprise an FKHR-like gene subfamily. *Genomics* 47: 187-199, 1998.
- Liu Y, Ao X, Ding W, Ponnusamy M, Wu W, Hao X, Yu W, Wang Y, Li P and Wang J: Critical role of FOXO3a in carcinogenesis. *Mol Cancer* 17: 104, 2018.
- Ai B, Kong X, Wang X, Zhang K, Yang X, Zhai J, Gao R, Qi Y, Wang J, Wang Z and Fang Y: LINC01355 suppresses breast cancer growth through FOXO3-mediated transcriptional repression of CCND1. *Cell Death Dis* 10: 502, 2019.
- Marlow LA, von Roemeling CA, Cooper SJ, Zhang Y, Rohl SD, Arora S, Gonzales IM, Azorsa DO, Reddi HV, Tun HW, *et al*: Foxo3a drives proliferation in anaplastic thyroid carcinoma through transcriptional regulation of cyclin A1: A paradigm shift that impacts current therapeutic strategies. *J Cell Sci* 125: 4253-4263, 2012.
- Yamamura Y, Lee WL, Inoue K, Ida H and Ito Y: RUNX3 cooperates with FoxO3a to induce apoptosis in gastric cancer cells. *J Biol Chem* 281: 5267-5276, 2006.
- Obexer P, Geiger K, Ambros PF, Meister B and Ausserlechner MJ: FKHL1-mediated expression of Noxa and Bim induces apoptosis via the mitochondria in neuroblastoma cells. *Cell Death Differ* 14: 534-547, 2007.
- Vandenberg CJ, Motoyama N and Cory S: FoxO3 suppresses Myc-driven lymphomagenesis. *Cell Death Dis* 6: e2046, 2016.
- Liu R and Jin JP: Calponin isoforms CNN1, CNN2 and CNN3: Regulators for actin cytoskeleton functions in smooth muscle and non-muscle cells. *Gene* 585: 143-153, 2016.
- She Y, Li C, Jiang T, Lei S, Zhou S, Shi H and Chen R: Knockdown of CNN3 impairs myoblast proliferation, differentiation, and protein synthesis via the mTOR pathway. *Front Physiol* 12: 659272, 2021.
- Daimon E, Shibukawa Y and Wada Y: Calponin 3 regulates stress fiber formation in dermal fibroblasts during wound healing. *Arch Dermatol Res* 305: 571-584, 2013.
- Dai F, Luo F, Zhou R, Zhou Q, Xu J, Zhang Z, Xiao J and Song L: Calponin 3 is associated with poor prognosis and regulates proliferation and metastasis in osteosarcoma. *Aging (Albany NY)* 12: 14037-14049, 2020.
- Yang C, Zhu S, Feng W and Chen X: Calponin 3 suppresses proliferation, migration and invasion of non-small cell lung cancer cells. *Oncol Lett* 22: 634, 2021.
- Otto T and Sicinski P: Cell cycle proteins as promising targets in cancer therapy. *Nat Rev Cancer* 17: 93-115, 2017.
- Malumbres M and Barbacid M: Cell cycle, CDKs and cancer: A changing paradigm. *Nat Rev Cancer* 9: 153-166, 2009.
- Malumbres M and Barbacid M: To cycle or not to cycle: A critical decision in cancer. *Nat Rev Cancer* 1: 222-231, 2001.
- Sherr CJ and Roberts JM: Living with or without cyclins and cyclin-dependent kinases. *Genes Dev* 18: 2699-2711, 2004.
- Hengartner MO: Apoptosis: Corraling the corpses. *Cell* 104: 325-328, 2001.

42. Schneider P and Tschopp J: Apoptosis induced by death receptors. *Pharm Acta Helv* 74: 281-286, 2000.
43. Danial NN and Korsmeyer SJ: Cell death: Critical control points. *Cell* 116: 205-219, 2004.
44. Ghobrial IM, Witzig TE and Adjei AA: Targeting apoptosis pathways in cancer therapy. *CA Cancer J Clin* 55: 178-194, 2005.
45. Amé JC, Spenlehauer C and de Murcia G: The PARP superfamily. *Bioessays* 26: 882-893, 2004.
46. Koh DW, Dawson TM and Dawson VL: Mediation of cell death by poly(ADP-ribose) polymerase-1. *Pharmacol Res* 52: 5-14, 2005.
47. Tewari M, Quan LT, O'Rourke K, Desnoyers S, Zeng Z, Beidler DR, Poirier GG, Salvesen GS and Dixit VM: Yama/ CPP32 beta, a mammalian homolog of CED-3, is a CrmA-inhibitable protease that cleaves the death substrate poly(ADP-ribose) polymerase. *Cell* 81: 801-809, 1995.
48. van Engeland M, Nieland LJ, Ramaekers FC, Schutte B and Reutelingsperger CP: Annexin V-affinity assay: A review on an apoptosis detection system based on phosphatidylserine exposure. *Cytometry* 31: 1-9, 1998.
49. Rosenwald A, Wright G, Chan WC, Connors JM, Campo E, Fisher RI, Gascoyne RD, Muller-Hermelink HK, Smeland EB, Giltane JM, *et al*: The use of molecular profiling to predict survival after chemotherapy for diffuse large-B-cell lymphoma. *N Engl J Med* 346: 1937-1947, 2002.
50. Lenz G, Wright G, Dave SS, Xiao W, Powell J, Zhao H, Xu W, Tan B, Goldschmidt N, Iqbal J, *et al*: Stromal gene signatures in large-B-cell lymphomas. *N Engl J Med* 359: 2313-2323, 2008.
51. Scott DW, Mottok A, Ennishi D, Wright GW, Farinha P, Ben-Neriah S, Kridel R, Barry GS, Hother C, Abrisqueta P, *et al*: Prognostic significance of diffuse large B-cell lymphoma cell of origin determined by digital gene expression in formalin-fixed paraffin-embedded tissue biopsies. *J Clin Oncol* 33: 2848-2856, 2015.
52. Sehn LH and Salles G: Diffuse large B-cell lymphoma. *N Engl J Med* 384: 842-858, 2021.



This work is licensed under a Creative Commons Attribution-NonCommercial-NoDerivatives 4.0 International (CC BY-NC-ND 4.0) License.